Diurnal variability of water vapour in the Baltic Sea region according to NCEP-CFSR and BaltAn65+ reanalyses*

doi:10.5697/oc.56-2.191
OCEANOLOGIA, 56 (2), 2014.
pp. 191–204.

© *Copyright by Polish Academy of Sciences, Institute of Oceanology, 2014.*

KEYWORDS
Precipitable water
Diurnal variability
Sea breeze
NCEP-CFSR
BaltAn65+

Erko Jakobson[1,2,⋆]
Hannes Keernik[1,2]
Andres Luhamaa[2,3]
Hanno Ohvril[2]

[1] Tartu Observatory,
61602 Tõravere, Tartumaa, Estonia;

e-mail: erko.jakobson@ut.ee

⋆corresponding author

[2] Institute of Physics,
University of Tartu,
Ülikooli 18, Tartu 50090, Estonia

[3] Estonian Meteorological and Hydrological Institute,
Mustamäe tee 33, Tallinn, Estonia

Received 25 October 2013, revised 12 March 2014, accepted 24 March 2014.

Abstract

Diurnal variations in water vapour in the Baltic Sea region are examined using BaltAn65+ and NCEP-CFSR reanalyses of summer (JJA) data for the period

* The survey was supported by the Estonian Science Foundation under a postdoctoral grant JD189, by European Social Fund's Doctoral Studies and Internationalisation Programme DoRa and project SLOOM12073T, which are carried out by the Archimedes Foundation, and by the Estonian Radiation Climate project, funded by the European Regional Development Fund.

The complete text of the paper is available at http://www.iopan.gda.pl/oceanologia/

1979–2005. A systematic difference between precipitable water (PW) diurnal variability above the land and the water is revealed. Above the land, PW diurnal variability has minimal values at 00 and 06 UTC, as in previous studies, whereas above the water, the minima are at 12 and 18 UTC. Diurnal variability in the vertical humidity profile is controlled by turbulent mixing and the diurnal behaviour of sea breezes. The impacts and proportions of diurnal variability of humidity are evaluated at different vertical levels.

1. Introduction

Water vapour, one of the most important variable components of the Earth's atmosphere, contributes on average about 60% of the natural greenhouse effect (Kiehl & Trenberth 1997, Maurellis & Tennyson 2003). The resource of cloud formation and precipitation, it plays a critical role in aerosol evolution and chemical reactions. Therefore, its column quantity must be adequately known in order to understand, associate and forecast environmental processes. On the other hand, temporal as well as spatial variability of water vapour occurs on such a fine scale that resolving them adequately presupposes observing systems with a high sampling resolution in space and time (Anthes 1983, Bengtsson et al. 2003).

Assimilated information from numerical weather prediction models and reanalyses are important tools for monitoring changes in integrated (total) water vapour content (precipitable water – PW), especially in areas, where the scarcity of observing systems restricts investigation (e.g. seas, large lakes, polar regions).

The diurnal variability of water vapour results from interactions between evaporation at the surface, atmospheric large-scale horizontal motion, moisture convergence and precipitation as well as vertical mixing (Dai et al. 1999a,b). The last-mentioned has almost no effect on PW but does contribute to evaporation in the lower layers. In addition, the diurnal PW cycle is affected by changes in local winds, which in coastal areas, in turn, depends on the sea breeze circulation (Dai et al. 2002, Ortiz de Galisteo et al. 2011). However, a sea breeze's regional ability to transport air between sea and land can be suppressed by atmospheric circulation on a larger scale (Arritt 1993). For the above-mentioned reasons, dependence on seasonality and geographical location should be considered when studying daily variations of PW.

As far as the Baltic Sea region is concerned, the diurnal cycle of PW was studied by Bouma & Stoew (2001), who evaluated GPS data from 30 European sites during a 2.5-year period. An average peak-to-peak (PtP) value between 0.8–3.2 mm for summer months (JAS) was found, which had a notable relationship with latitude. However, the maximum value phase

of the diurnal cycle does not depend on latitude and occurs at about 14–17 UTC. Eliminating sites below 55°N and extending the study period to 6 years, the average diurnal PtP converged to 0.1–0.6 mm (Bouma 2002). As in these papers, diurnal variations in PW in the Baltic region during a 10-year period (1996–2005) were analysed by Jakobson et al. (2009). Averaged over 32 land-located GPS stations, the maximum PW in summer (JJA) occurred at 14 UTC with an average diurnal PtP-value of just 0.64 mm. For spring (MAM) the average PtP-value was 0.51 mm. In both spring and summer, all 32 GPS stations, without exception, showed higher PW values at 12 UTC compared to 00 UTC. The average PtP-value was only 0.16 mm in the autumn and 0.11 mm in the winter. The authors concluded that it seemed reasonable to neglect the diurnal cycles in PW during the autumn and winter seasons. We believe that the discrepancy among the PtP-values in Bouma & Stoew (2001), Bouma (2002) and Jakobson et al. (2009) arises from the Bouma & Stoew (2001) paper, in which the PtP-values relate to only a short 2.5-year period, where the synoptic variations in PW were not sufficiently smoothed out.

Okulov & Ohvril (2010) obtained a contrary result about PW diurnal behaviour at the coastal station Tallinn-Harku (59.48°N, 24.60°E, 1990–2001): at midnight (00 UTC) PW is 3–5% higher than its midday (12 UTC) counterpart.

To investigate the reasons for the PW diurnal cycle in more detail, one needs to retrieve the diurnal evolution of the humidity profile. Apart from using models, this has only been done by intensive radiosonde campaigns (e.g. Dai et al. 2002) or, more recently, by GPS tomography (e.g. Bastin et al. 2007). However, these methods are limited by the low temporal and horizontal resolution (radiosonde) or the sparse network (GPS tomography).

Another shortcoming of these methods is the location of sites, namely, the absence of stationary radiosonde and GPS stations on the Baltic Sea. In this sense, the databases created by atmospheric reanalysis models represent powerful modern tools securing sufficient temporal and spatial resolution for detecting regional diurnal cycles in the vertical profiles of meteorological elements.

The authors of this paper are not aware of any study applying a reanalysis-based approach to the determination of PW diurnal variability.

The aims of this paper are to establish the average summer (JJA) PW diurnal variability above the water as well as the land, and also to ascertain the atmospheric layers responsible for this variability. Diurnal temperature, specific humidity and wind profiles will also be examined.

2. Material and methods

Our research is based on two extensive databases. The first one, completed for the 31-year period from 1979 to 2010, was provided by the global atmospheric reanalysis model from the National Centre of Environmental Predictions – Climate Forecast System Reanalysis (NCEP-CFSR, USA). It has a 0.5-degree horizontal, 64-layer vertical and 6-hour temporal resolution and takes account of most available in situ and satellite observations (Saha et al. 2010). The second model used in this study, completed for the 41-year period from 1965 to 2005, is the regional reanalysis model BaltAn65+, which is based on HIRLAM version 7.1.4; it has a 0.1-degree horizontal, 60-layer vertical and 6-hour temporal resolution (Luhamaa et al. 2010). The BaltAn65+ obtains boundary fields from ECMWF ERA-40 global reanalyses, assimilating standard surface observations and meteorological soundings together with ship and buoy measurements from the WMO observational network. As a refinement of ERA-40 for Baltic Sea region, the BaltAn65+ has improved its resolution: using a >10 times higher horizontal resolution than ERA-40, it is suitable for studying such a heterogeneous region as the Baltic Sea, which is characterised by variable landscapes, indented coastlines, numerous islands and rich inland waters.

The study area of this paper is 53–68°N, 12–32°E, which means that local time is from 48 minutes to 2 hours 8 minutes behind UTC time. Owing to the relatively small interval, compared to models with a 6-hour resolution, all calculations are still done in UTC-time.

The motivation for preferring these reanalysis models was to select the most independent models available, so as to reduce the risk of model-generated artificial patterns. Both models assimilated mostly the same data, but their physical parameterisation schemes are different. Data for the overlapping period 1979–2005 from NCEP-CFSR and BaltAn65+ were analysed. The BaltAn65+ data from 1965–1978 were omitted in order to keep the periods closer and to avoid systematic errors that ERA-40 had before the satellite era (Jakobson & Vihma 2010). NCEP-CFSR data from 2006–2010 were left out, so that only data from the same period would be compared.

3. Results

All the diurnal differences shown in the figures (except Figure 4, see p. 197) are statistically significant ($p<0.05$), based on the t-test; insignificant differences are left blank.

BaltAn65+ summer (JJA) average PW has an evident latitudinal dependence (Figure 1) with an orographic effect over the Scandinavian Mountains. However, there is no visual correlation with the underlying surface type. The overall summer average PW over the region was 20.7 mm, while local average values of PW varied from 13.1 mm to 23.9 mm.

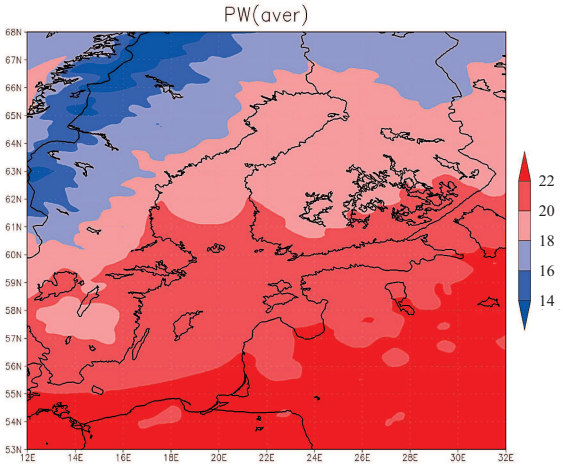

Figure 1. Precipitable water (PW, mm): summer (JJA) average for 1979–2005 from NCEP-CFSR reanalysis

The differences between the average 12 UTC and 00 UTC values of PW are shown in Figure 2. Based on the properties of the underlying surface, systematic patterns in PW diurnal variability are evident and are roughly the same in both models. The diurnal variability of PW above the Baltic Sea and above the land behaves in the opposite way according to both of

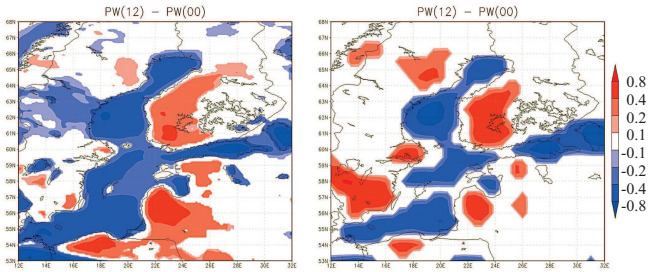

Figure 2. Summer (JJA) difference in precipitable water, $PW_{12\,UTC} - PW_{00\,UTC}$ in mm: left-hand panel – BaltAn65+ for 1979–2005; right-hand panel – NCEP-CFSR for 1979–2005

the models – above the sea there is usually more water vapour at 00 UTC, compared to the land at 12 UTC. According to the BaltAn65+ model, the average PW over the sea is 0.5 mm higher at 00 UTC than at 12 UTC, while over the land there is no difference between the average PW values at 00 UTC and 12 UTC.

A noteworthy difference between the models appears if we take the larger lakes and islands into consideration. The BaltAn65+ model tends to classify larger islands (Saaremaa, Gotland) as land and larger lakes (Ladoga, Vänern, Peipus, Vättern) as water. Of these, the NCEP-CFSR model detects only Lake Ladoga, presumably because of the sparser resolution of the model.

The diurnal evolution of PW, with a 6-hour time step, is shown in Figure 3. At night, from 00 to 06 UTC, there is no change in PW above the sea, but a decrease above the land is detectable. In the morning, from 06 to 12 UTC, PW decreases above the sea, but increases above the land, especially to the east of the Baltic Sea.

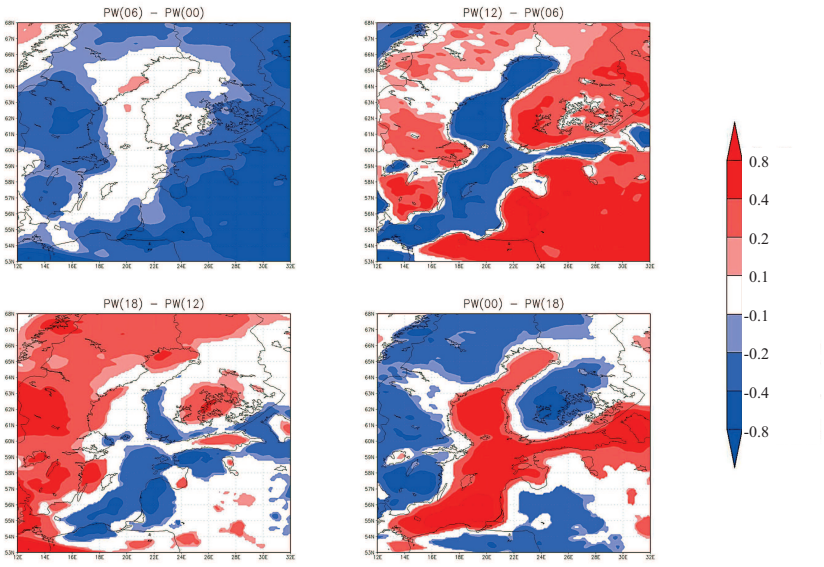

Figure 3. Summer (JJA) differences in precipitable water, PW [mm], as calculated from BaltAn65+ for 1979–2005 between different UTC hours

In the afternoon, from 12 to 18 UTC, PW still decreases slightly above the water, except in the Gulf of Finland and on Lake Ladoga, where PW is already increasing, as is the case to the west of the Baltic Sea. In the evening, from 18 to 00 UTC, PW is increasing above the water, but is mostly decreasing above the land.

For the sake of comparison with previous studies (Bouma & Stoew 2001, Jakobson et al. 2009), shorter periods were also processed, but because of the insufficient number of data, the diurnal differences remained mostly insignificant (not shown), without any justifiable opportunity for making comparisons.

To estimate the influence of different atmospheric layers on PW diurnal variation, the PW difference between 18 and 06 UTC ($dPW = PW_{18\ UTC} - PW_{06\ UTC}$) was calculated, as this time interval usually gives the largest differences in PW. After that, the contributions to dPW from vertical intervals 900–1000 hPa, 800–900 hPa and 800–1000 hPa were calculated (Figure 4). Lower 100 hPa humidity diurnal variations affect PW diurnal variability more above the water than the land, while the 800 to 900 hPa interval affects it more above land than the water. Relatively speaking, the regional average contribution to dPW was 25% in the interval 900–1000 hPa and 45% in the next 100 hPa layer. The 800–1000 hPa interval holds 70% of the dPW with a ca 20% larger contribution above the land than over the sea.

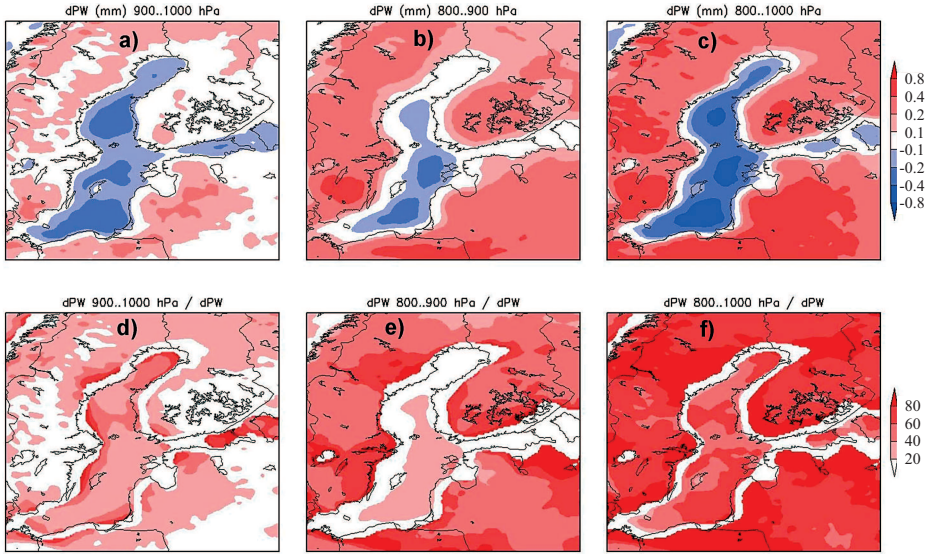

Figure 4. Contributions of different vertical intervals to precipitable water; PW difference between 18 and 06 UTC, calculated from BaltAn65+ for 1979–2005. The first row represents the absolute [mm] and the second row the relative [%] contribution to the PW difference from the relevant vertical interval a, d) 900–1000 hPa; b, e) 800–900 hPa; c, f) 800–1000 hPa

Specific humidity and temperature at 00, 06, 12 and 18 UTC differ from their diurnal average values at different vertical pressure levels and exhibit

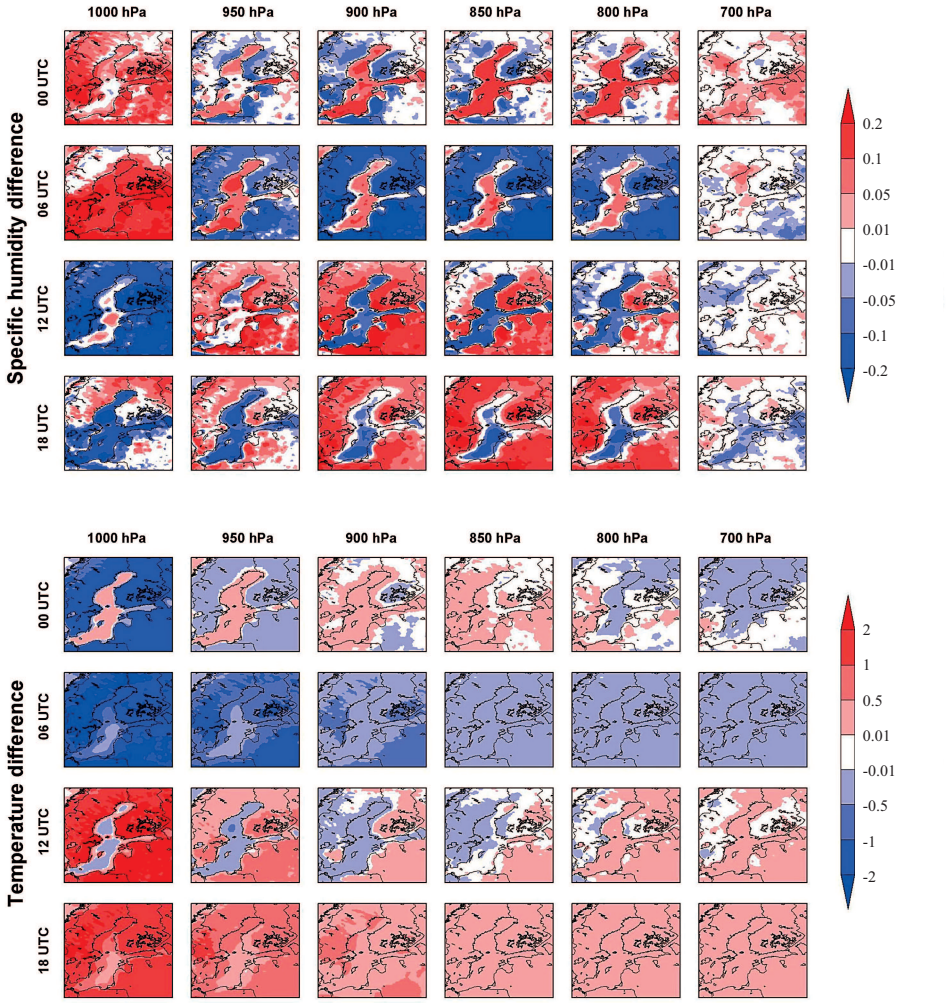

Figure 5. Upper panel – specific humidity [g kg^{-1}] at 00, 06, 12 and 18 UTC minus the average specific humidity; lower panel – temperature [°C] at 00, 06, 12 and 18 UTC the minus average temperature. Rows – hours; columns – pressure levels. Data from BaltAn65+ for 1979–2005

fundamental differences for the sea and the land (Figure 5). The results for BaltAn65+ and NCEP-CFSR (not shown) were similar at all vertical levels with respect to both specific humidity and temperature. The behaviour of specific humidity above 950 hPa is the reverse of that above the sea and the land. Above the sea there is less humidity at 12 and 18 UTC, while above the land the humidity is lower at 00 and 06 UTC. The situation regarding the specific humidity below 950 hPa is more complicated and will be analysed in the Discussion. Over land, temperatures are higher at 18 and 12 UTC and

lower at 06 and 00 UTC. Diurnal variability in the temperature above the water is delayed for about 6 hours, compared to the variability above the land, with higher temperatures at 18 and 00 UTC and lower temperatures at 06 and 12 UTC, although the delay fades out above 850 hPa.

Figure 6 presents the winds at 00 and 12 UTC minus the relevant diurnal averages at 1000, 950 and 900 hPa. At the 1000 hPa level there is a distinct land breeze at 00 UTC and a sea breeze at 12 UTC on the Baltic Sea and also on the larger lakes (Ladoga and Vänern). At 950 hPa the breeze effect is still weakly present, but already at 900 hPa the breeze effects are no longer apparent.

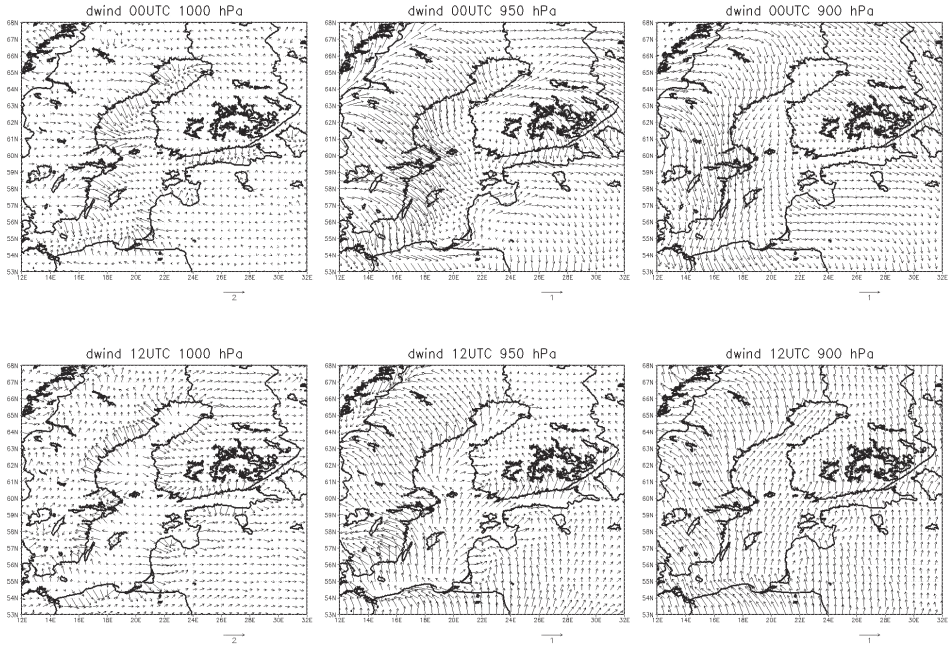

Figure 6. Upper panels – wind at 00 UTC minus the diurnal average; lower panels – wind at 12 UTC minus the diurnal average. The columns represent pressure levels of 1000, 950 and 900 hPa

4. Discussion

There are three mechanisms that can change the humidity content in the atmosphere: 1) large-scale (synoptic) changes of the air mass; 2) evaporation and condensation within the air mass; and 3) local wind-driven advection. The large-scale changes in the synoptic situation do not follow a diurnal pattern, as they are caused by large-scale changes of the air mass and can be

compensated for by averaging over long time periods. Nonetheless, air mass changes affect PW behaviour much more than other inducers, so studies of PW diurnal variability using intensive but short measuring periods (for example, Wu et al. 2003, Bastin et al. 2007) are likely to be affected by the air mass changes. The other two mechanisms are both related to the diurnal cycle of solar radiation (Wu et al. 2003). The diurnal cycle of solar radiation drives the humidity cycle via the temperature cycle. Diurnal warming intensifies evaporation and increases humidity. Also, warmer air can contain more moisture. The diurnal cycle of solar radiation also generates sea/land breezes as result of the differential warming of land and water. During daytime in summer, the water is colder than the land and the sea breeze carries moisture inland. During the night in summer, the water is warmer than the air and the land breeze carries air from land to water. After sunrise, surface warming above the land triggers convective turbulence and vertical mixing of air. The extent of the mixed layer increases with the intensity of the incident solar radiation and is also driven by the type of underlying surface and the pattern of its albedo. Convective turbulence carries moisture from the lower layers upwards and upper drier air downwards, favouring evaporation from the surface.

4.1. Diurnal variability of temperature, specific humidity and PW above the land

At night (00 UTC) the atmosphere cools off below 900 hPa; above that level the change in temperature is mostly insignificant. As there is less evaporation and turbulent mixing, the specific humidity also decreases in the whole profile, compared to the situation 6 hours earlier, causing the decrease in PW.

In the morning (06 UTC) the temperature decreases in the entire column. The specific humidity increases below 950 hPa, and this is often accompanied by radiative fog (ground fog) and dew, which entrains water vapour and reduces column humidity, i.e. PW. Because of the downward transport of water vapour, the specific humidity decreases above 950 hPa.

By noon (12 UTC) the temperature has increased in the whole profile, especially below 950 hPa. The specific humidity increases above 950 hPa, but decreases below that. This can be explained by the upward convective transport of humidity in the first 1 km layer. As a daily average, the difference in specific humidity between 1000 hPa and 900 hPa is about 1.5 g kg^{-1} (not shown). As a result of mixing, the lowermost layers lose humidity, while the uppermost ones gain it. PW increases, especially east of the Baltic Sea.

In the evening (18 UTC) the temperature remains the same below 950 hPa, but increases above that. The specific humidity increases at 1000 hPa, but remains the same above that. The evening increase in the lowermost level can be explained by the weakening of turbulent mixing, so humidity generated by evaporation at ground level remains mostly at the lowermost levels. PW has remained the same east of the Baltic Sea, but has increased to the west.

4.2. Diurnal variability of temperature, specific humidity and PW above the water

The average PW diurnal variability above the water, in contrast to the land, reaches minimum values at 12 to 18 UTC and maximum values at 00 UTC. The origin of this disparity is in the breezes – the sea breeze during the day and the land breeze at night. During the day, the sea breeze brings colder air in off the sea to the land at very low levels, but this rises after warming and returns aloft towards the sea where it eventually descends to close the cycle.

The night-time land breeze cycle is the reverse of the day-time sea breeze one, with air ascending over the sea and descending above the land. During the day, descending air brings drier air from the upper air levels and thus reduces PW. During the night, ascending air flow above the water transports humid air up and increases PW. The diurnal variabilities in specific humidity and temperature at different atmospheric levels are also forced by the sea/land breezes.

At night (00 UTC) the temperature decreases slightly, but is still higher than the diurnal average. The land breeze carries humidity upwards, increasing PW. By morning (06 UTC) the temperature has decreased in the whole profile. The specific humidity has increased below 950 hPa level, presumably due to the very high relative humidity that occurs with morning fogs, but has decreased above the 950 hPa level, apparently due to the downward-moving water droplets. PW does not change significantly from 00 to 06 UTC.

By noon (12 UTC) the temperature has slightly increased in the whole profile, but it is still lower than the diurnal average. The specific humidity has decreased in the whole profile. Above the water, descending drier air in sea breeze leads to a decrease in specific humidity in the whole profile and in PW. In the evening (18 UTC) the temperature continues to increase in the whole profile. The specific humidity decreases below 950 hPa, but increases above that. In the lowermost layers, the sea breeze blocks the humid air from the land, but in the uppermost layers the returning air in the sea breeze carries humidity above the water. The diurnal minimum of

specific humidity (Figure 5) and PW decreases towards the Baltic Proper. PW increases in the Gulf of Finland and Lake Ladoga, probably because of their smaller dimensions.

5. Conclusions

The diurnal cycle of PW has already been studied using radiosonde and GPS measurement data (Bouma & Stoew 2001, Dai et al. 2002, Jakobson et al. 2009). All of these measurements were performed on land, not on water. However, our results, based on atmospheric reanalysis models, are in a good agreement with them. But the agreement addresses only land, where the diurnal cycle of PW has a maximum in the afternoon. Although all land-located 32 GPS-stations revealed a similar PW diurnal cycle (Jakobson et al. 2009), one cannot generalise these results to the regions adjoining large water bodies (the Baltic Sea, large lakes). Our results from the reanalysis models demonstrated (Figure 3) that above the water the PW diurnal variability is the reverse of the variability above the land. Near water minimum PW values occur at 12 and 18 UTC and maximum ones at 00 and 06 UTC. The difference is caused by sea/land breezes at lower altitudes (Figure 6).

The main regularities in the humidity and temperature profiles of the Baltic Sea region are as follows:

Above the land:

- Diurnal variability of specific humidity above 950 hPa is coherent with the diurnal variability of temperature with minimum values at 00 and 06 UTC and maximum ones at 12 and 18 UTC. Below 950 hPa the specific humidity maximum is at 06 UTC, presumably due to the very high relative humidity occur with morning fogs, and the minimum is at 12 UTC because convective turbulent mixing transports drier air from higher to lower levels.
- PW diurnal variability is also coherent with the diurnal variability of temperature, with minimum values at 00 and 06 UTC and maximum ones at 12 and 18 UTC.
- 60% of PW diurnal variability is controlled by humidity diurnal variations in the vertical interval 800–900 hPa and 80% at 800–1000 hPa.

Above the water (sea, lakes):

- The main inducers above the sea are the sea breeze during the daytime with its descending airflow, and the land breeze at night with

ascending air; minimum values are at 12 and 18 UTC, and maximum ones at 00 and 06 UTC.

- PW diurnal variability falls to a minimum at noon, from 12 to 18 UTC, and rises to a maximum at night from 00 to 06 UTC.
- 40% of PW diurnal variability is controlled by diurnal variations in humidity at the vertical interval 900–1000 hPa and 60% at 800–1000 hPa.

Acknowledgements

We thank the NCEP and BaltAn65+ teams for supplying the data.

References

Anthes R. A., 1983, *Regional models of the atmosphere in middle latitudes*, Mon. Weather Rev., 111 (6), 1306–1335, http://dx.doi.org/10.1175/1520-0493(1983)111<1306:RMOTAI>2.0.CO;2.

Arritt R. W., 1993, *Effects of the large scale flow on characteristics features of the sea breeze*, J. Appl. Meteorol., 32 (1), 116–125, http://dx.doi.org/10.1175/1520-0450(1993)032<0116:EOTLSF>2.0.CO;2.

Bastin S., Champollion C., Bock O., Drobinski P., Masson F., 2007, *Diurnal cycle of water vapor as documented by a dense GPS network in a coastal area during ESCOMPTE IOP2*, J. Appl. Meteorol. Clim., 46 (2), 167–182, http://dx.doi.org/10.1175/JAM2450.1.

Bengtsson L., Robinson G., Anthes R., Aonashi K., Dodson A., Elgered G., Gendt G., Gurney R., Jietai M., Mitchell C., Mlaki M., Rhodin G., Silverstrin P., Ware R., Watson R., Wergen W., 2003, *The use of GPS measurements for water vapor determination*, B. Am. Meteor. Soc., 84 (9), 1249–1258, http://dx.doi.org/10.1175/BAMS-84-9-1249.

Bouma H. R., Stoew B., 2001, *GPS observations of daily variations in the atmospheric water vapor content*, Phys. Chem. Earth, 26 (A6-8), 389–392.

Bouma H. R., 2002, *Ground-based GPS in climate research*, Tech. Rep. No. 456L, Licentiate Thesis, School Environ. Sci. School Electric. Eng., Chalmers Univ. of Tech., Göteborg.

Dai A., Giorgi F., Trenberth K. E., 1999a, *Observed and model-simulated precipitation diurnal cycle over the contiguous United States*, J. Geophys. Res., 104 (D6), 6377–6402, http://dx.doi.org/10.1029/98JD02720.

Dai A., Trenberth K. E., Karl T. R., 1999b, *Effects of clouds, soil moisture, precipitation and water vapor on diurnal temperature range*, J. Climate, 12 (8), 2451–2473, http://dx.doi.org/10.1175/1520-0442(1999)012<2451:EOCSMP>2.0.CO;2.

Dai A., Wang J., Ware R., Van Hove T., 2002, *Diurnal variation in water vapor over North America and its implications for sampling errors in radiosonde*

humidity, J. Geophys. Res., 107 (D10), ACL 11-1–ACL 11-14, http://dx.doi.org/10.1029/2001JD000642.

Jakobson E., Ohvril H., Elgered G., 2009, *Diurnal variability of precipitable water in the Baltic region, impact on transmittance of the direct solar radiation*, Boreal Environ. Res., 14 (1), 45–55.

Jakobson E., Vihma T., 2010, *Atmospheric moisture budget over the Arctic on the basis of the ERA-40 reanalysis*, Int. J. Climatol., 30 (14), 2175–2194, http://dx.doi.org/10.1002/joc.2039.

Kiehl J. T., Trenberth K. E., 1997, *Earth's annual global mean energy budget*, B. Am. Meteorol. Soc., 78 (2), 197–208, http://dx.doi.org/10.1175/1520-0477(1997)078<0197:EAGMEB>2.0.CO;2.

Luhamaa A., Kimmel K., Männik A., Rõõm R., 2010, *High resolution re-analysis for the Baltic Sea region during 1965–2005 period*, Clim. Dynam., 36 (3–4), 727–738, http://dx.doi.org/10.1007/s00382-010-0842-y.

Maurellis A. N., Tennyson J., 2003, *The climatic effects of water vapour*, Phys. World, 16 (5), 29–33.

Okulov O., Ohvril H., 2010, *Column transparency and precipitable water in Estonia. Variability during the last decades*, Lambert Acad. Publ., Saarbrücken, 69 pp.

Ortiz de Galisteo J. P., Cachorro V., Toledano C., Torres B., Laulainen N., Bennouna Y., de Frutos A., 2011, *Diurnal cycle of precipitable water vapor over Spain*, Q. J. Roy. Meteor. Soc., 137 (657), 948–958, http://dx.doi.org/10.1002/qj.811.

Saha S., Moorthi S., Pan H.-L., Wu X., Wang J., Nadiga S., Tripp P., Kistler R., Woollen J., Behringer D., Liu H., Stokes D., Grumbine R., Gayno G., Wang J., Hou Y.-T., Chuang H.-Y., Juang H.-M. H., Sela J., Iredell M., Treadon R., Kleist D., Van Delst P., Keyser D., Derber J., Ek M., Meng J., Wei H., Yang R., Lord s., Van Den Dool H., Kumar A., Wang W., Long C., Chelliah M., Xue Y., Huang B., Schemm J.-K., Ebisuzaki W., Lin R., Xie P., Chen M., Zhou S., Higgins W., Zou C.-Z., Liu Q., Chen Y., Han Y., Cucurull L., Reynolds R. W., Rutledge G., Goldberg M., 2010, *The NCEP climate forecast system reanalysis*, B. Am. Meteorol. Soc., 91 (8), 1015–1057, http://dx.doi.org/10.1175/2010BAMS3001.1.

Wu P., Hamada J., Mori S., Tauhid Y. I., Yamanaka M. D., Kimura F., 2003, *Diurnal variation of precipitable water over a mountainous area of Sumatra Island*, J. Appl. Meteorol., 42, 1107–1115, http://dx.doi.org/10.1175/1520-0450(2003)042<1107:DVOPWO>2.0.CO;2.